

## Numerical Forecasting of Radiation Fog. Part I: Numerical Model and Sensitivity Tests

THIERRY BERGOT\* AND DANIEL GUEDALIA

*Laboratoire d'Aerologie, Université Paul Sabatier, Toulouse, France*

(Manuscript received 4 October 1991, in final form 25 October 1993)

### ABSTRACT

To improve the forecast of dense radiative fogs, a method has been developed using a one-dimensional model of the nocturnal boundary layer forced by the mesoscale fields provided by a 3D limited-area operational model. The 1D model involves a treatment of soil-atmosphere exchanges and a parameterization of turbulence in stable layers in order to correctly simulate the nocturnal atmospheric cooling.

Various sensitivity tests have been carried out to evaluate the influence of the main input parameters of the model (geostrophic wind, horizontal advections, cloud cover, soil moisture, etc.) on the predicted fog characteristics. The principal result concerns the difficulty of obtaining accurate forecasts in the case of fog appearing in the middle or at the end of the night, when the local atmospheric cooling is weak.

### 1. Introduction

Fog, and more particularly dense fog, is a meteorological phenomenon that greatly affect air and road transport. If cooling is the main physical mechanism involved in its formation, the fog is referred to as a radiation fog (of the kind generally formed during nocturnal cooling above continental surfaces). On the other hand, fog caused mainly by humidification is called "advection fog" (e.g., fog in coastal areas or over the sea).

Several fog research programs have been conducted over the last 20 years. Some observation programs in the 1970s increased our knowledge of the processes involved in fog formation. The first program was developed by the UK Meteorological Office (UKMO) on the Cardington site (Roach 1976; Roach et al. 1976, 1982). Observations made on the site revealed the role of turbulence in fog formation, as well as changes in the vertical profile of the wind, and the quasi-periodical oscillations at the top of the fog layer. Another program was developed by the Atmospheric Sciences Research Center-State University of New York (ASRC-SUNY) in Albany, New York, between 1977 and 1981 (Jiusto and Lala 1980, 1983). The measurements taken at Albany helped increase our knowledge of fog but also demonstrated the complexity of processes involved in

the formation and evolution of a fog layer, as well as its dependence on mesoscale conditions (Lala et al. 1982). Very detailed observations of fog were also made on the Cabauw site (the Netherlands) by means of a 215-m-high tower (Duykerke 1991b).

More recently in France, the Laboratoire d'Aerologie, acting in the framework of the Fog Research Group, made a series of observations on sites equipped with towers in Valladolid, Spain, in 1985 (Moneris 1989; Guedalia et al. 1989) and in Carnin, France, from 1988 (Guedalia and Bergot 1992).

Fog formation forecasting by meteorological services using operational models has not made much progress in recent years. Indeed, fog forecasting requires an adequate representation of the nocturnal boundary layer (radiative cooling near the surface and turbulence in stratified layers), a high-resolution vertical grid close to the surface (fog rarely exceeds 100 m in height), and a parameterization of soil-atmosphere interactions. Finally small-scale surface heterogeneities add to the difficulties.

Several 1D models have been developed for fog prediction. Among the first, one might mention that of Zdunkowski and Nielsen (1969), which did not take into account sedimentation of the liquid water nor exchange coefficient parameterization; this model was later improved (Zdunkowski and Barr 1972) by introducing a calculation of exchange coefficients. Brown and Roach (1976) used a model that was more suitable for fog and that was later refined by Turton and Brown (1987) using new parameterization for nocturnal exchange coefficients. These authors pointed out that a major problem in reproducing the observations had to do with the fact that the advection was not taken into account. Finally, and more recently, we should mention

\* Current affiliation: Smirn/Meteo-France, Villeneuve d'Ascq, France.

Corresponding author address: Dr. Daniel Guedalia, Laboratoire d'Aerologie, Université Paul Sabatier, 118 route de Narbonne, 31062, Toulouse, France.

the Duynkerke model (1991a), which, in addition to the physical parameterization necessary for a detailed description of the NBL, includes a representation of soil-vegetation-atmosphere exchanges. Advection, however, is not taken into account.

We know of at least one attempt to use a mesoscale model in fog forecasting made by the UKMO. This model uses cloud water content as a prognostic variable and with sufficiently sophisticated physics for use in fog forecasting. It was used to simulate the case of fog formed over the Atlantic Ocean and advected onto north Scotland (Ballard et al. 1991). The main conclusion of this study was that correct initialization (of fog already formed) was indispensable in order to then be able to predict the diurnal evolution of this maritime fog. No test of continental radiation fog prediction has been published using this model.

It is clear that fog forecasting will always be difficult, as fog is a "threshold phenomenon." The time at which condensation begins and hence the humidity and temperature of the lower layers of the atmosphere have to be predicted with great precision. Furthermore, all previous studies have shown that the problems of surface heterogeneities and horizontal advection have to be taken into account. Two approaches are possible. The first requires forecasting by means of a mesoscale model able to include surface heterogeneities, advections, etc., with high horizontal and vertical resolution. We have already mentioned the work of Ballard et al. (1991) in the UKMO; other projects are likely to emerge in other meteorological services in other countries. Nevertheless, this method requires a great deal of computing time. The second method consists of using a 1D model forced with mesoscale terms (geostrophic wind and horizontal advections). This method can be used only in regions without orography and with weak surface heterogeneity, as the 1D model is not able to take these into account. This approach was first used by Musson-Genon (1987), who recommended a 1D model forced by advections resulting from a general circulation forecasting model.

The method described here makes use of the Musson-Genon idea. The 1D model used is derived from the nocturnal boundary layer model of Laboratoire d'Aerologie, which has been used successfully to simulate nocturnal situations (Estournel and Guedalia 1985; Estournel 1988). As with the Duynkerke model (1991a), it uses exchange coefficient parameterization for stable stratification layers; dew and frost deposition are also taken into account. The mesoscale forcing is given by the French PERIDOT limited-area forecasting model (35-km horizontal grid).

In this paper we present the model and a set of sensitivity tests made in order to study the influence of errors in input parameters (initial conditions, geostrophic wind, advection, etc.) on the forecasting of fog formation and development. This method of forcing a 1D model with mesoscale fields was developed for use

in the Nord-Pas de Calais region (between Paris and the French-Belgian border), which is frequently subjected to fog but relatively homogeneous. Different simulations of real cases, corresponding to observations made on the Carnin site, in the center of the region, for the purpose of testing the method's reliability are presented in Part II.

## 2. The COBEL one-dimensional model of radiation fog

The COBEL (Couche Brouillard Eau Liquide) model is derived from the 1D model of the nocturnal boundary layer developed by the Laboratoire d'Aerologie of the Toulouse University (Estournel 1988). The main characteristics of this model are (i) a turbulent mixing parameterization adapted to strong stable stratification, (ii) a high spectral resolution longwave radiative scheme, (iii) an implicit parameterization for microphysics, and (iv) a coupling between the soil and the atmosphere for heat exchanges and dew (or frost) deposition.

### a. Model formulation

The equations are derived from the Reynolds system with the Boussinesq hypothesis:

$$\frac{\partial u}{\partial t} = f(v - v_g) - \frac{\partial \overline{w'u'}}{\partial z} \tag{1}$$

$$\frac{\partial v}{\partial t} = -f(u - u_g) - \frac{\partial \overline{w'v'}}{\partial z} \tag{2}$$

$$\frac{\partial \theta}{\partial t} = -\frac{\partial \overline{w'\theta'}}{\partial z} + \frac{\theta}{T} \left( \frac{1}{\rho c_p} \frac{\partial F_r}{\partial z} + \frac{L}{c_p} C \right) + Adv\theta \tag{3}$$

$$\frac{\partial q}{\partial t} = -\frac{\partial \overline{w'q'}}{\partial z} - C + Advq, \tag{4}$$

where  $f$  is the Coriolis parameter,  $u$  and  $v$  the orthogonal components of the horizontal wind,  $\theta$  the potential temperature,  $T$  the temperature, and  $q$  the humidity mixing ratio;  $\overline{w'\alpha'}$  represents the turbulent flux of quantity  $\alpha$ ,  $F_r$  the net radiative flux,  $C$  the condensation rate by air mass unit,  $c_p$  the specific heat of air at constant pressure,  $L$  the latent heat of evaporation, and  $\rho$  the air density.

The orthogonal components of geostrophic winds ( $u_g$  and  $v_g$ ) and the horizontal thermal ( $Adv\theta$ ) and humidity ( $Advq$ ) advection are external forcing terms.

### b. Turbulent closure

The turbulent closure is certainly the most important point of a 1D boundary-layer model. The turbulent transport is recognized as a major factor for fog formation and evolution, and an accurate representation of stable layers is necessary in the case of fog models. The closure selected here is at the order 1.5. The tur-

bulent fluxes are related to the vertical gradients by means of an exchange coefficient:

$$w'\alpha' = -K_\alpha \frac{\partial \alpha}{\partial z}, \quad \text{for } \alpha = u, v, \theta, q. \quad (5)$$

The turbulent diffusion coefficients  $K_\alpha$  are given in terms of stability dependent mixing length  $l_\alpha$  and the turbulent kinetic energy  $E_k$ :

$$K_\alpha = C_\alpha l_\alpha E_k^{1/2}, \quad (6)$$

where  $C_\alpha$  is a constant value taken equal to 0.4.

The following equation allows us to calculate the time evolution of turbulent kinetic energy:

$$\frac{\partial E_k}{\partial t} = -\frac{\overline{\partial w' E_k'}}{\partial z} - \overline{u' w'} \frac{\partial u}{\partial z} - \overline{v' w'} \frac{\partial v}{\partial z} + \frac{g}{T} \overline{w' \theta'} - \epsilon, \quad (7)$$

where  $g$  is the gravity acceleration and  $\epsilon$  the kinetic energy dissipation.

Various parameterizations of the mixing length  $l_\alpha$  have been used for boundary-layer modeling (Delage 1974; Therry and Lacarrere 1983; Bougeault and André 1986). Most of these parameterizations have been checked under daytime or weak instability conditions, and their application to the case of strong stable nocturnal layers is less obvious. (They predict a critical Richardson number at which turbulence ceases.)

Some fog models take the problem of strong stability into account. Thus, Turton and Brown (1987), who, after Yamada (1983), took a residual value for the exchange coefficient for Ri taken between 0.16 and 0.89. Duynkerke (1991a) uses a specific relation for the values of  $z/L$  greater than 1. We have used the relation suggested by Estournel and Guedalia (1987) deduced from observations of the nocturnal stable layers. This relation is

$$l_\alpha = \begin{cases} l_n(1 - 5 \text{ Ri}), & \text{Ri} \leq 0.16 \\ l_n(1 + 41 \text{ Ri})^{-0.84}, & \text{Ri} > 0.16, \end{cases} \quad (8)$$

where Ri is the Richardson number and  $l_n$  is the neutral mixing length, expressed as (Delage 1974)

$$l_n = \frac{kz}{1 + (kz/G_n)}, \quad (10)$$

where  $k$  is the von Kármán constant and  $G_n = 4 \times 10^{-4} u_g f^{-1}$ .

These relations have been checked against experimental data in the case of stable nocturnal layers (Estournel 1988; Monerris 1989). In the cases of unstable layers we have used the mixing length relation proposed by Bougeault and Andre (1986):

$$\int_z^{z+L_{\text{up}}} \beta[\theta(z') - \theta(z)] dz' = E_k(z), \quad (11)$$

$$\int_{z-L_{\text{down}}}^z \beta[\theta(z) - \theta(z')] dz' = E_k(z), \quad (12)$$

$$l_\alpha = \min(L_{\text{down}}, L_{\text{up}}). \quad (13)$$

In the presence of liquid water, the Brunt-Väisälä frequency  $N^2$  introduced into Ri calculation is computed from

$$N^2 = \frac{g}{T} \left( \frac{dT}{dz} + \Gamma_m \right), \quad (14)$$

where  $\Gamma_m$  is the saturated adiabatic lapse rate. Durran and Klemp (1982) showed that relation (14) represents a good approximation of the expression of  $N^2$  in a saturated atmosphere.

### c. Radiative transfer

#### 1) SHORTWAVE RADIATION

The daily variation of the net solar flux ( $\lambda < 4 \mu\text{m}$ ) at the surface is assigned; this flux intensity is used to compute the surface temperature [see (21)].

#### 2) LONGWAVE RADIATION

For longwave radiation (4–100  $\mu\text{m}$ ), the scheme used is exactly similar to the one described by Vehil et al. (1988) for studies of the nocturnal boundary layer (NBL). It is a high-resolution spectral model (232 spectral ranges) that allows us to calculate the net radiative flux at each level of the model grid. This very complete radiation scheme had been used in the NBL model. A simplified version of this scheme will be used in the final version of the forecasting model in order to reduce the computing time.

The radiative effect of liquid water droplets is calculated within the atmospheric window (8–12  $\mu\text{m}$ ). The scattering is neglected in the calculation of the optical depth of fog. Taking into account the size of fog droplets (radii less than 15  $\mu\text{m}$ ), one may consider a linear relationship between the liquid water content in the fog ( $q_l$ ) and the optical depth  $\delta$  (for  $\lambda = 10 \mu\text{m}$ ):

$$\delta(\Delta Z) = k_1 q_l \Delta Z. \quad (15)$$

We have used the value  $k_1 = 149.5$ , checked by Gerther and Steele (1980).

#### 3) THE RADIATIVE EFFECT OF CLOUDS

The presence of clouds increases the value of the downward longwave flux received at the surface and therefore decreases the cooling rate (Brown and Roach 1976). So, the model also has a downward longwave “cloudy flux” at the top; this cloudy flux corresponds to the blackbody emission at the mean temperature of

the cloud, and it is computed only in the atmospheric window.

*d. Parameterization of the microphysics*

As noted above, the scheme used in the present work is an implicit parameterization. As soon as the mixing ratio  $q$  reaches the saturation value  $q_{sat}$ , the excess condenses as liquid water  $q_l$ . The equilibrium temperature  $T^*$  and mixing ratio  $q^*$  are then calculated. The energy and the total water content ( $q + q_l$ ) are thus conserved:

$$c_p T + Lq = c_p T^* + Lq^* \tag{16}$$

$$q^* = q_{sat}(T^*).$$

The equation for time evolution of the liquid water is

$$\frac{\partial q_l}{\partial t} = \frac{\partial}{\partial z} \left( K_z \frac{\partial q_l}{\partial z} \right) + \frac{\partial G}{\partial z} + C. \tag{17}$$

The main difficulty lies in determining the gravitational settling flux  $G$ . According to Brown and Roach (1976),  $G$  can be expressed as follows:

$$G = v_i q_l, \tag{18}$$

where  $v_i$  is the settling velocity. It depends exclusively on the shape of the droplet size distribution, which is not known in the model. Some authors have postulated the shape of a gamma function for this spectrum (Turton and Brown 1987; Duynkerke 1991a). Other authors have suggested formulas based on experimental drop size distributions:  $v_i = 62.5 \times 10^2 q_l$  (Brown and Roach 1976);  $v_i = 1.9$  (Kunkel 1984), where  $v_i$  is in centimeters per second, and  $q_l$  in kilograms per kilogram.

The data collected during dense radiation fogs in the fog field study Lille 88 (Guedalia and Bergot 1992) have shown that the shape of the drop size distribution (at the 1.5-m altitude) rapidly reaches an equilibrium. Hence, the settling velocity is near constant during the whole phase of mature fog. Furthermore, due to the vertical mixing in a dense fog layer, the drop size distribution is uniform with the altitude. Consequently, a parameterization of the type  $v_i$  being constant is used. The problem is then to determine this constant value. The influence of an error on the settling velocity on the development of the fog is analyzed in the sensitivity study paragraph.

The horizontal visibility is computed from the liquid water content by the relation

$$vis = \frac{3.9}{144.7(\rho q_l)^{0.88}}. \tag{19}$$

*e. The soil-atmosphere exchanges*

The exchanges between the soil and the atmosphere are represented by a thermal coupling and by the dew and frost flux at the ground. The soil is represented by

five levels between the surface and a depth of 1 m. The equation of the temperature evolution into the soil is

$$\frac{\partial T_s}{\partial t} = \frac{\partial}{\partial z} \left( \frac{K_s}{\rho_s c_{ps}} \frac{\partial T_s}{\partial z} \right), \tag{20}$$

where  $K_s$  is the thermal conductivity coefficient,  $\rho_s$  the volumic mass, and  $C_{ps}$  the heat capacity of the soil. The surface temperature  $T_0$  is determined from the energetic budget at ground level:

$$F_{IR} + F_{vis} - \epsilon_0 \sigma T_0^4 + H_{atm} + H_{sol} + LE_g = 0, \tag{21}$$

where  $F_{IR}$  and  $F_{vis}$  are the downward longwave and net shortwave flux at ground level, respectively,  $\epsilon_0$  the emissivity of the soil,  $H_{atm}$  the atmospheric sensible heat flux,  $H_{sol}$  the heat flux inside the soil, and  $LE_g$  the atmospheric latent flux.

In nocturnal conditions, the hydric exchanges between the soil and the atmosphere mainly concern the dew and frost deposition. This deposition reduces the humidity of the air in close proximity to the ground surface, which tends to delay the formation of the fog. Therefore, the parameterization of the dew flux is a very important question in a fog model. The dew flux is expressed from the evaporation relation

$$E_g = \rho C_h [q_a - hu q_{sat}(T_0)], \tag{22}$$

where  $q_a$  is the mixing ratio at the first atmospheric level,  $q_{sat}(T_0)$  the saturated mixing ratio at ground level,  $hu$  a coefficient taking into account the humidity of the soil, and  $C_h$  a drag coefficient. The quantity  $hu$  depends on the amount of liquid water within the soil surface layer. For the dew flux calculation,  $hu = 1$  (Noilhan and Planton 1989).

The frost deposition is of greater importance than the dew deposition and may play a role in delaying fog formation (Turton and Brown 1987). To compute this effect, we have introduced a new parameter  $hu_{frost}$ :

$$hu_{frost} = hu \frac{e_{ices}(T_0)}{e_{ws}(T_0)}, \tag{23}$$

where  $e_{ices}$  is the saturated value over ice and  $e_{ws}$  is the saturated value over liquid water.

Despite the high resolution of the vertical grid near the surface, the logarithmic profile shape implies that the gradients required to calculate the coefficient  $C_h$  are not well defined, so  $C_h$  value for stable stratification is taken from Pielke (1984):

$$C_h = \frac{ku_*}{0.74[\ln(z/z_0) + 6.35z/L_{MO}]}, \tag{24}$$

where  $L_{MO}$  is the Monin-Obukkov length,  $u_*$  the friction velocity, and  $z_0$  the roughness length equal to 3 cm.

*f. Boundary conditions and vertical grid*

At the top of the model (1400 m), the turbulent flux for  $\theta$  and  $q$  are zero;  $u = u_g$  and  $v = v_g$ . At the lower

boundary the wind is set to zero and the temperature at the depth of 1 m in the soil is constant.

Equations (1), (2), (3), (4), (7), (17), and (20) are solved by a finite-difference method. The vertical grid involves 30 levels distributed in a log-linear arrangement between the ground and 1400 m, and five additional levels in the soil between the surface and a depth of 1 m. The grid increment is minimum close to the surface in such a way to follow the surface cooling and the development of the fog. (The first atmospheric level is at 0.5 m and the second is at 1.65 m, whereas the first level into the soil is at 0.05 m.)

### 3. Sensitivity study

The main purpose of our method of dense fog forecasting is to be able to resolve the following problems: the first is to determine the time of fog formation, and the second is to determine its characteristics and in particular the horizontal visibility and height of the fog layer.

Before doing real-case simulations (these will be dealt with in Part II), we carried out a sensitivity study in order to determine how uncertainty concerning the model's input parameters would affect the quality of fog forecasting.

The atmospheric conditions favorable for fog formation are found in an anticyclonic situation with moderate winds and clear sky. In the case of a nocturnal layer with moderate wind, the cooling of the atmosphere near the ground involves two phases: during the first few hours, the cooling is very significant ( $2^{\circ}$ – $5^{\circ}\text{C h}^{-1}$ ), and then during the rest of the night it is low or almost negligible ( $<0.5^{\circ}\text{C h}^{-1}$ ). So one may expect the influence of input parameters to be different according to whether the fog forms at the beginning or at the end of the night.

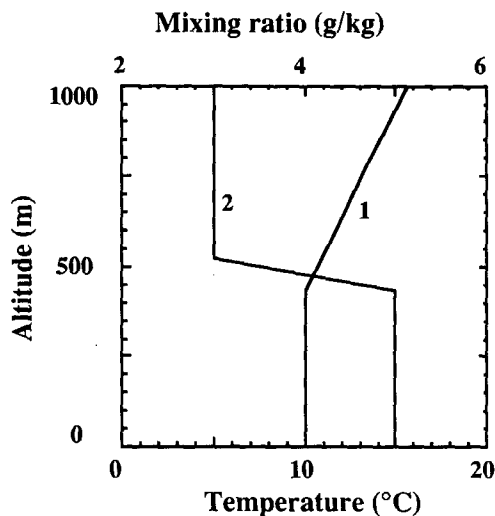


FIG. 1. Standard initial conditions for temperature (curve 1) and mixing ratio (curve 2).

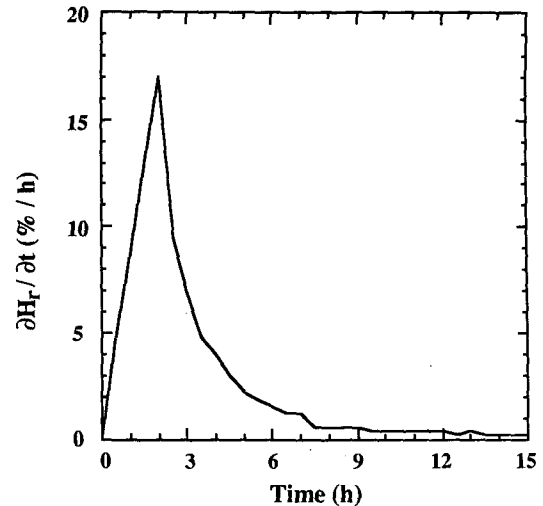


FIG. 2. Variation rate of relative humidity ( $\% \text{ h}^{-1}$ ) at 1-m altitude as a function of time in a clear-sky night. Initial time corresponds to the beginning of the cooling.

To study the sensitivity of the model to different input parameters, we conducted a series of simulations with the 1D model; the mesoscale forcing terms (horizontal gradients and geostrophic wind) were directly imposed. The time step was 60 s before condensation and 30 s afterward. The radiative calculation was done every 15 min. The soil parameters ( $k_s = 1 \text{ W K}^{-1} \text{ m}^{-1}$  and  $\rho_s c_p = 2 \times 10^6 \text{ J K}^{-1} \text{ m}^{-3}$ ) correspond to the winter season.

The initial conditions correspond to a neutral atmosphere—that is, in winter, approximately 2 h prior to sunset. The mixing layer, in which temperature and mixing ratio are uniform, is 500 m thick (Fig. 1). The neutral wind profile is computed from the geostrophic wind. The variation of the surface solar flux corresponds to that of the month of December, at  $50^{\circ}\text{N}$ .

#### a. Initial conditions sensitivity

Several previous works have shown that the choice of initial conditions is a determinant element in fog simulation (Musson-Genon 1987; Fitzjarrald and Lala 1990; Ballard et al. 1991; etc.) and, more particularly, the values of temperature and humidity of the surface layer. The model was initialized under neutral conditions corresponding to the afternoon boundary layer, before the start of nocturnal cooling. Three initializing parameters were therefore necessary: the height of the mixing layer and the temperature and humidity values in this layer—in other words, the relative humidity. We first tested the effect of a variation on the value of the height of the initial mixing layer. We initialized successively with heights of 250, 500, and 1000 m; the effect is very weak, which may be explained by the fact that the thickness of radiation fog rarely exceeds 100 m.

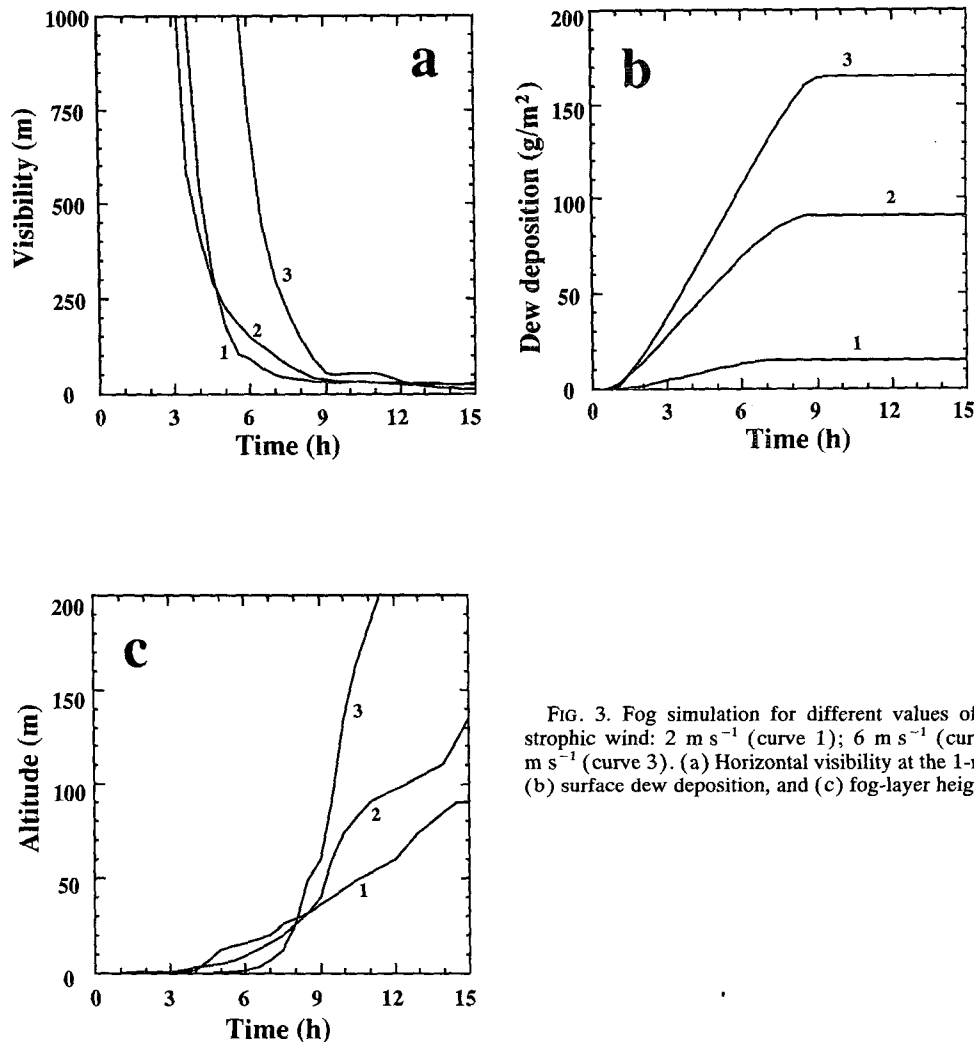


FIG. 3. Fog simulation for different values of the geostrophic wind: 2 m s<sup>-1</sup> (curve 1); 6 m s<sup>-1</sup> (curve 2); 10 m s<sup>-1</sup> (curve 3). (a) Horizontal visibility at the 1-m altitude, (b) surface dew deposition, and (c) fog-layer height.

We then studied the effect of an error in the initial value of the temperature or humidity on the time of fog formation. Next we calculated, for the case of a winter night with moderate wind, the time variation in the relative humidity of the atmosphere, a result of nocturnal cooling and dew deposition (Fig. 2). The relative humidity increases significantly during the first 3–4 h, and then very slightly.

A precision of 2°C (temperature) and of 0.5 g kg<sup>-1</sup> (mixing ratio) would appear to be necessary for the situations where fog that forms at the beginning of the night and from 5°C and 0.1 g kg<sup>-1</sup> for fog that forms late in the night, if one wishes to obtain a precision of the order of 1 h in the time of fog formation. Obviously, these values are only orders of magnitude, which depend on the atmospheric cooling conditions.

Finally, the most difficult case is when the fog forms at the end of the night ( $H$ , less than 60%), since a small

initial error may or may not result in fog formation. Analysis of these typical cases shows how important it is to know the precise initial relative humidity, especially in the case of fog, which is likely to form during the second half of the night.

#### b. Geostrophic wind sensitivity

During the nocturnal phase, the value of the geostrophic wind has an influence on the atmospheric turbulence near the surface (Estourel 1988; Estourel and Guedalia 1985). When the geostrophic wind increases, the height of the nocturnal inversion is greater but surface cooling is lower because of the increase in turbulent downward fluxes of sensible heat.

Concerning the physical processes, some fundamental differences occur according to the intensity of the geostrophic wind. Under strong wind conditions the

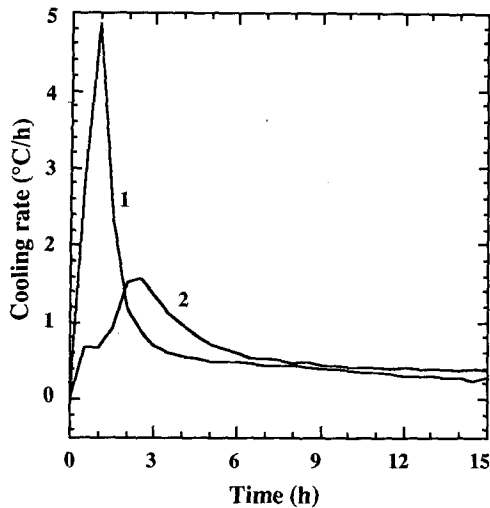


FIG. 4. Local (turbulent and radiative) atmospheric cooling rate in a clear-sky night case at the 1-m (curve 1) and 25-m (curve 2) altitudes.

dew deposition is greater; the radiative cooling of the atmosphere is lower (the temperature profile curvature is less marked than for moderate winds), and the turbulent cooling, on the other hand, is greater. We see that all of the processes have opposite effects, which explains why the literature on the effect of turbulence on fog is so controversial.

We carried out different simulations, under identical initial conditions ( $T = 10^{\circ}\text{C}$  and  $q = 6 \text{ g kg}^{-1}$ ), with a geostrophic wind taken between 2 and  $10 \text{ m s}^{-1}$ . In Fig. 3a we see that there is not much difference between the time of fog formation for winds taken between 2 and  $6 \text{ m s}^{-1}$  and that, on the other hand, fog forms 2 h later when  $U_g = 10 \text{ m s}^{-1}$ . The differences are clearer when condensation occurs later in the night; in this case the influence of the dew deposition is still very significant (Fig. 3b). It may be seen that it is greater to the extent that the wind is strong, which tends to postpone the time of fog formation. The geostrophic wind also affects the height of fog (Fig. 3c). We may sum up the effect of the geostrophic wind by saying that the stronger it is, the more the time of fog formation will be postponed (the fog may even be prevented from forming) but once formed, its vertical development will be increased by the wind. This seems to demonstrate that the errors that might be expected in the value of the geostrophic wind will not have a significant effect on the time of fog formation.

### c. Horizontal advection sensitivity

Vertical exchanges are less significant during the night than during the day, and it is important to determine the influence of horizontal advection on fog formation and evolution. Turton and Brown (1987) had already pointed out the difficulty of correctly simulat-

ing the cases observed if advection is not taken into account. The respective effects of a temperature or humidity advection on fog are fairly similar: a cold advection has a similar effect as a positive humidity advection. Consequently, we shall describe only the study with a temperature advection.

We assume that the horizontal temperature gradient is constant between the surface and a height of 100 m and that it decreases beyond that until it reaches the zero value at 450 m. During the night, because of the stable stratification, there is always a wind speed vertical gradient in the inversion layer, and as a result there is also a vertical gradient for thermal advection. For example, if we assume a horizontal gradient of  $1^{\circ}\text{C}$

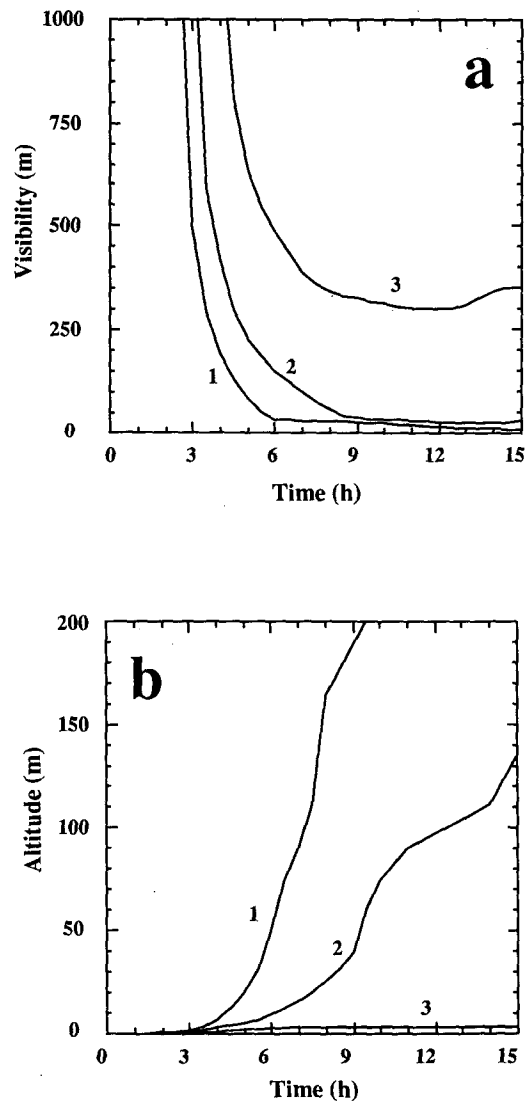


FIG. 5. Fog simulation (initial  $q = 6 \text{ g kg}^{-1}$ ) with a thermal advection of  $1^{\circ}\text{C} (100 \text{ km})^{-1}$ . Cool advection (curve 1), without advection (curve 2), and warm advection (curve 3). (a) Horizontal visibility at 1 m; (b) fog-layer height.

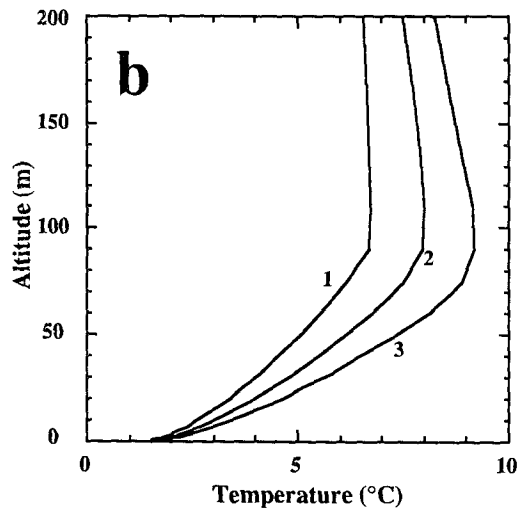
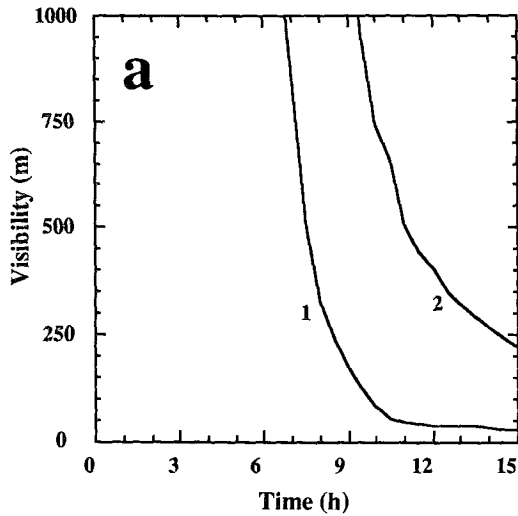


FIG. 6. (a) Same as Fig. 5 except initial  $q = 5 \text{ g kg}^{-1}$ , and (b) vertical temperature profile after 6 h of simulation.

$(100 \text{ km})^{-1}$ , with a geostrophic wind of  $6 \text{ m s}^{-1}$ , the thermal advection will be  $0.04^\circ\text{C h}^{-1}$  at 1.5 m and  $0.24^\circ\text{C h}^{-1}$  at 50 m; for  $u_g = 2 \text{ m s}^{-1}$ , the values will be  $0.02^\circ\text{C h}^{-1}$  and  $0.11^\circ\text{C h}^{-1}$ , respectively.

For a greater understanding of the influence of advection on fog formation, it is useful to compare the rate of ‘‘local’’ cooling (turbulent and radiative) with advective cooling during the night (Fig. 4). We see that ‘‘local’’ cooling is greater at the beginning of the night and much greater than advective cooling. We carried out simulations with a warm or cold thermal advection of  $1^\circ\text{C} (100 \text{ km})^{-1}$ . Several cases have been considered: the first corresponds to a fog formation at the beginning of the night (initial  $q = 6 \text{ g kg}^{-1}$ ). The time of fog formation is not changed with a cold ad-

vection but a warm advection delays the fog formation by 1 h (Fig. 5a). On the other hand, the advection has a strong effect on fog development (Fig. 5b): the situation with cold advection results in a fog with very rapid vertical growth.

The same simulations done with an initial mixing ratio of  $5 \text{ g kg}^{-1}$  (with the goal of forming the fog later in the night) gave different results. In this case, the rate of advective cooling is not negligible with respect to the rate of local cooling, and depending on whether the advection is warm or cold, the corresponding times of fog formation differ by several hours (Fig. 6a).

To conclude, advection has a very significant effect on the vertical development of fog; this influence is due mainly to the fact that advection during the night is greater in the upper part of the inversion layer than in

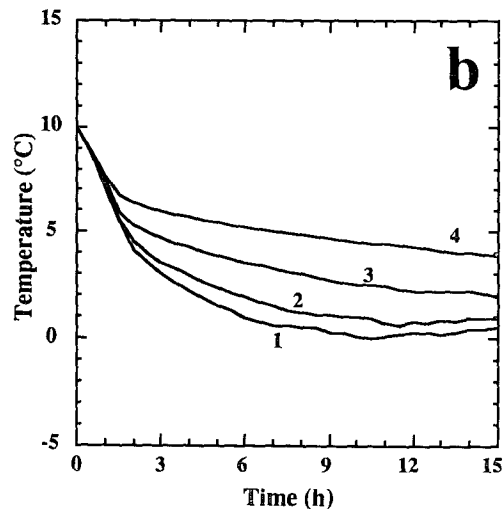
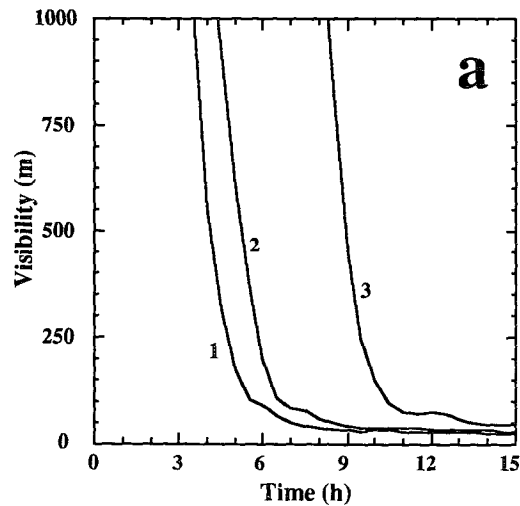


FIG. 7. Fog simulation with a constant cloud cover. Cloudy flux value ( $\text{W m}^{-2}$ ): clear sky (curve 1), 10 (curve 2), 30 (curve 3), and 50 (curve 4). (a) Horizontal visibility at 1 m; (b) time evolution of temperature at 1 m.



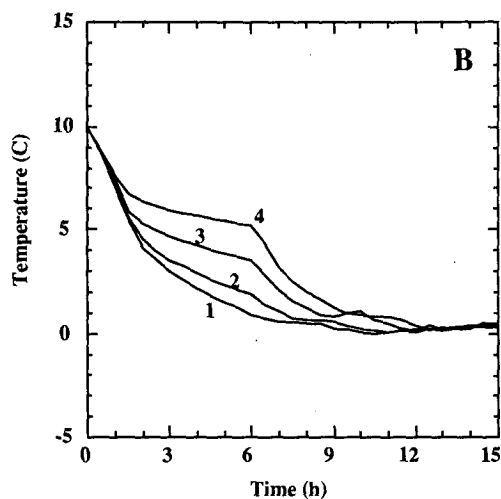
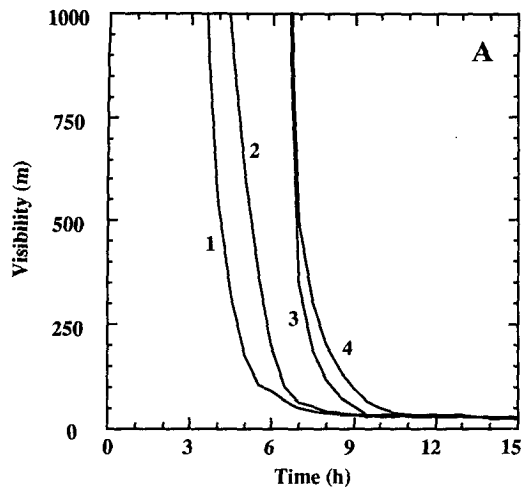


FIG. 8. Same as Fig. 7 except dissipation of cloud cover after 6 h of simulation.

its lower part (Fig. 6b). The existence of thermal advection can significantly change the time of fog formation if the fog is formed during the second half of the night. Fitzjarrald and Lala (1989) had already pointed out the effect of advection on the height of fogs observed in the Hudson Valley.

#### d. Cloud cover sensitivity

The presence of clouds modifies the value of infrared flux received at the surface and consequently the rate of atmospheric cooling. The increase of infrared flux, called "cloudy flux," typically varies between  $10 \text{ W m}^{-2}$  (the case for cirrus) and up to  $50 \text{ W m}^{-2}$  (the case for stratocumulus).

In the case of a homogeneous cloud cover that remains throughout the night, the atmospheric cooling will be slower. A cloudy flux of  $10$  or  $30 \text{ W m}^{-2}$  will delay fog formation by 1 or 5 h, respectively, whereas

a low cloud cover ( $50 \text{ W m}^{-2}$ ) will prevent fog formation (Fig. 7).

An interesting case is the one involving a change in the cloud cover during the night (appearance or dissipation). In a first case we simulated a cloud cover that disappeared 6.5 h after the beginning of the simulation. We observed (except for the cirrus) that when the clouds disappear, atmospheric cooling accelerates (Fig. 8b) and the fog forms 1 h after this disappearance (Fig. 8a). Finally, the last case studied was that of the arrival of a cloud layer during the night, 6 h after the beginning of the simulation, when the fog was already formed. Here again, a cirrus layer has no apparent effect, whereas a low cloud layer heats the atmosphere close to the surface (Fig. 9b), which causes attenuation of the fog (in the case of  $30 \text{ W m}^{-2}$ ) or even dissipation over several hours (in the case of  $50 \text{ W m}^{-2}$ ) (Fig. 9a).

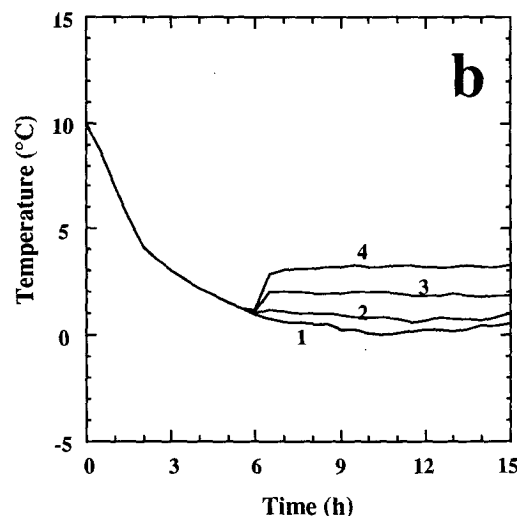
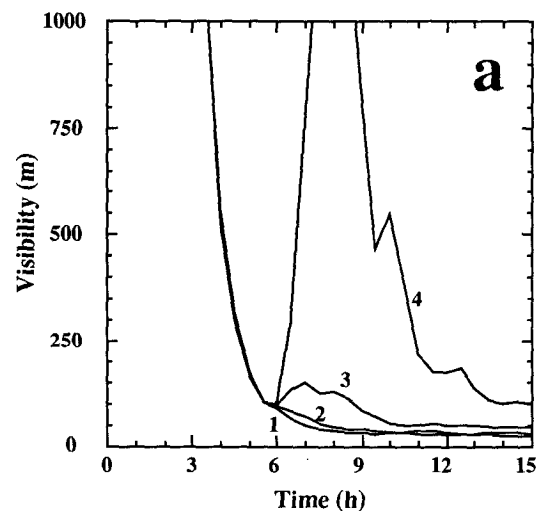


FIG. 9. Same as Fig. 7 except appearance of a cloud cover after 6 h of simulation.

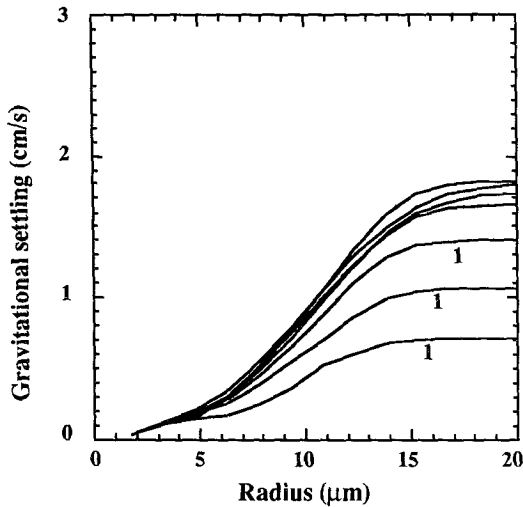


FIG. 10. Cumulative value of gravitational settling versus droplet radius. These values were deduced from droplet size distribution measured in a fog event on 21 November 1988 (Lille 88 experiment). The four upper curves were obtained in the fog mature phase between 0035 and 0430 UTC. The three curves marked with 1 were obtained in the fog dissipation phase between 0555 and 0745 UTC.

The results of these simulations show that for accurate forecasting of fog formation it is necessary to have an available estimate of the variation of the low- and midlevel clouds during the night.

*e. Gravitational settling sensitivity*

The knowledge of the value of the gravitational settling is essential in fog models. Experimental data obtained from dense fogs (Pinnick et al. 1978; Corradini et al. 1980; Guedalia and Bergot 1992) show that the droplet size distribution contains more small droplets during the formation phase and that during the “mature” fog phase the gravitational setting does not change very much. This may be seen in Fig. 10, which represents the gravitational setting values deduced from the droplet size distribution measured at height of 1.5 m during the Lille 88 field experiment. First of all, it is interesting to observe that the liquid water was contained in droplets with a radius less than 15  $\mu\text{m}$ . The gravitational setting values calculated were between 1.6 and 1.8  $\text{cm s}^{-1}$  during the dense fog phase and between 0.7 and 1.4  $\text{cm s}^{-1}$  during the dissipation phase, when there were fewer larger droplets.

We studied the effect of an error in the value of the gravitational setting on fog development. Three different values were used: 1  $\text{cm s}^{-1}$  (dissipation phase or fogs formed in a polluted atmosphere), and 1.5 and 2  $\text{cm s}^{-1}$  (limits taken for a dense fog). The error in the time of fog formation (horizontal visibility less than 1000 m) is less than 1 h regardless of the  $v_i$  value (Fig. 11a); on the other hand, the gravitational setting value has an effect on the liquid water content in the fog layer

(Fig. 11b). It may be observed that the differences obtained are greater between 1 and 1.5  $\text{cm s}^{-1}$  than between 1.5 and 2  $\text{cm s}^{-1}$ .

*f. Soil thermal conductivity sensitivity*

The thermal conductivity value will influence the rate of nocturnal cooling of the surface. For a given type of soil, this conductivity mainly depends on its moisture. A moist soil decreases the surface cooling rate and consequently delays the appearance of fog. In extreme cases, between a dry soil ( $K_s = 0.5$ ) and a moist soil ( $K_s = 1.5$ ), the difference in times of fog appearance may be as great as 8 h. But this difference

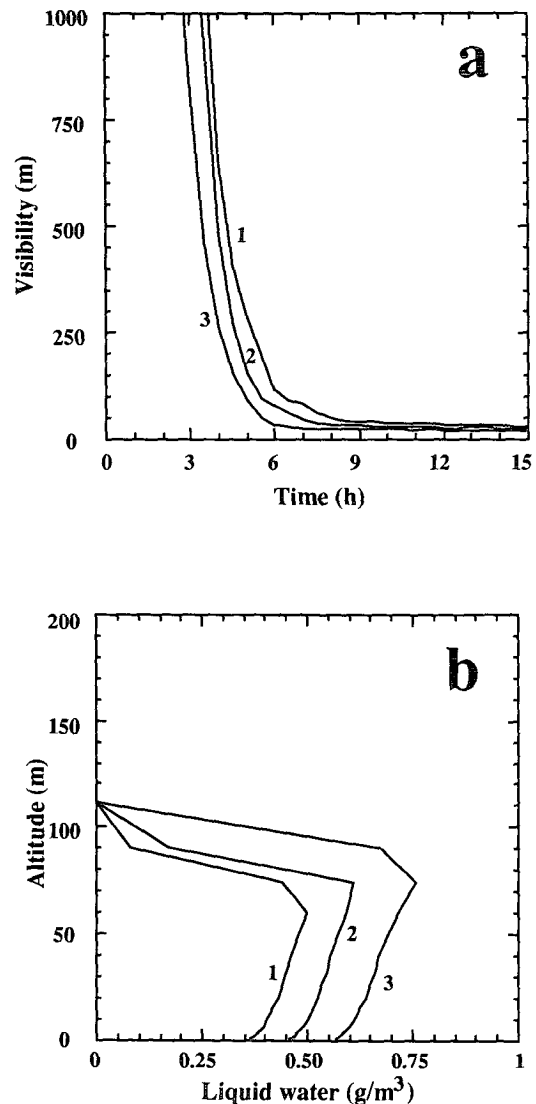


FIG. 11. Fog simulation for different values of gravitational settling: 2  $\text{cm s}^{-1}$  (curve 1), 1.5  $\text{cm s}^{-1}$  (curve 2), 1  $\text{cm s}^{-1}$  (curve 3). (a) Horizontal visibility at 1 m; (b) vertical profile of liquid water content.

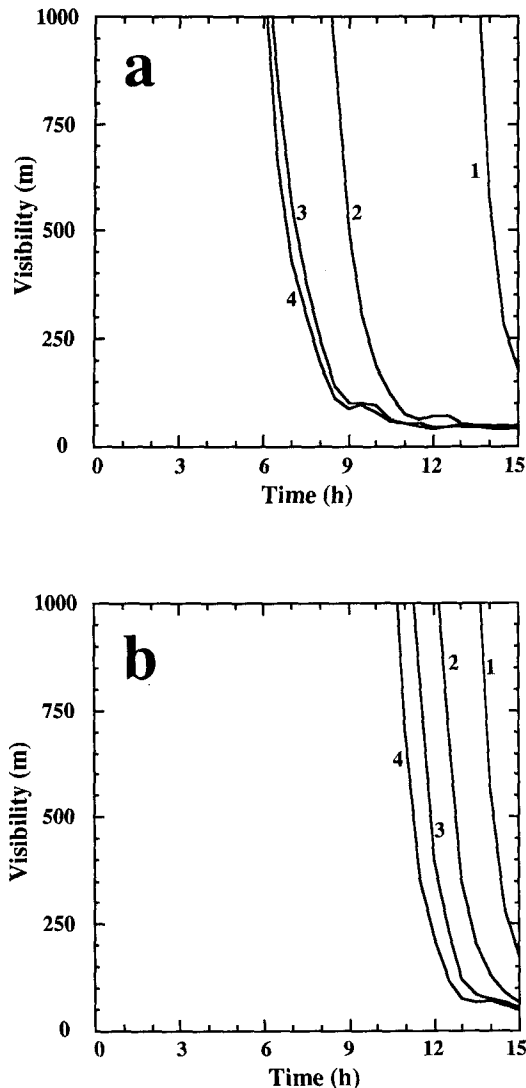


FIG. 12. Influence of the thermal conductivity of the soil on fog formation. (a) Homogeneous moist soil,  $K_s = 1.5$  (curve 1) and homogeneous dry soil,  $K_s = 0.5$  (curve 4). The other two curves correspond to a moist deep soil,  $K_s = 1.5$  with a superficial dry layer ( $K_s = 0.5$ ) within the first 5 cm (curve 2) or within the first 10 cm (curve 3). (b) Homogeneous moist soil,  $K_s = 1.5$  (curve 1) and homogeneous moderate moist soil,  $K_s = 1$  (curve 4). The other two curves correspond to a moist deep soil,  $K_s = 1.5$ , with a superficial moderate moist layer ( $K_s = 1$ ) within the first 5 cm (curve 2) or within the first 10 cm (curve 3).

will be only 3 h when changing from a moderately moist soil ( $K_s = 1$ ) to a very moist soil ( $K_s = 1.5$ ).

During the winter period, favorable for fog formation, the superficial soil layer (a few centimeters thick) is, because of wind and solar radiation, less moist than the deeper layers. It is therefore important to know the depth of the soil that will affect the thermal exchanges for a period of about 10–12 h. We carried out a series of simulations with a deep moist soil ( $K_s = 1.5$ ) and a drier superficial soil. It may be observed (Fig. 12) that

it is the thermal conductivity value of the 10 first centimeters of soil that affects the rate of surface cooling and that therefore needs to be precisely known.

#### g. Dew deposition sensitivity

In most nocturnal situations, dew or frost deposition on the surface precedes fog formation. This deposition, by decreasing the atmospheric water vapor content near the surface delays the appearance of fog. To reveal this effect, we compared the simulation results with and without dew deposition (Fig. 13a). It was observed that the dew deposition delayed the fog formation by 4 h.

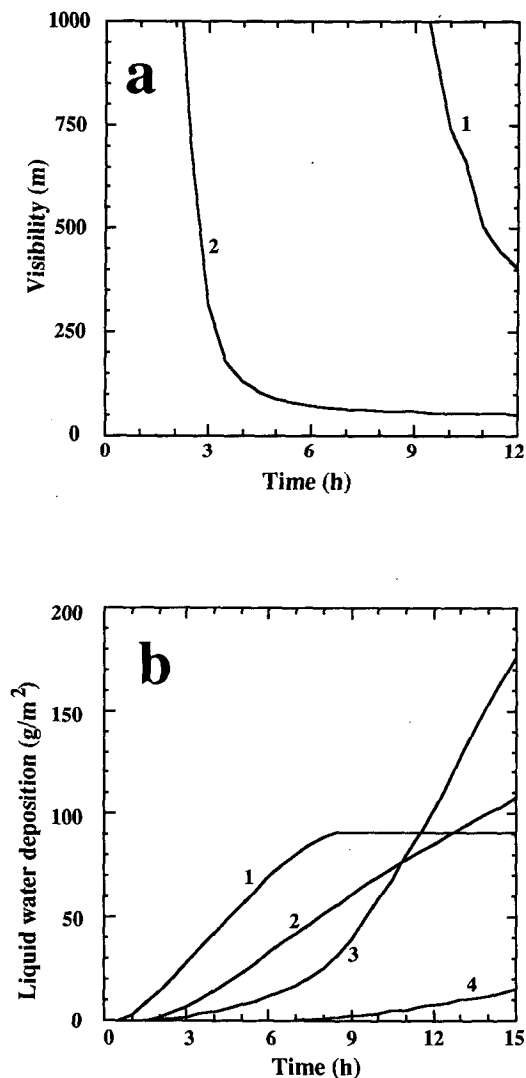


FIG. 13. Influence of dew deposition on fog formation. (a) Horizontal visibility at 1 m in the case of a simulation with (curve 1) or without (curve 2) dew deposition. (b) Fog formed at the beginning of the night (initial  $q = 6 \text{ g kg}^{-1}$ ): dew deposition (curve 1) and gravitational deposition (curve 2). Fog formed later in the night: dew deposition (curve 3) and gravitational deposition (curve 4).

It is interesting to compare dew deposition and liquid water deposition by gravitational setting (Fig. 13b). When the fog forms at the beginning of the night, the dew is the most significant; this dew deposition becomes zero at a certain time corresponding to the end of surface cooling (due to the increase of infrared flux emitted by the fog).

#### 4. Conclusions

In spite of the notable improvement of numerical models these last few years, fog forecast remains fairly difficult to achieve. Sophisticated numerical 1D boundary-layer models (Duykerke 1991a; Turton and Brown 1987; Estournel 1988) can now be successfully used to simulate evolution of the nocturnal layer and hence of fog. This approach is very suitable for situations with horizontal homogeneity (soil, relief, etc.) but comparison with observations shows that mesoscale circulation linked to horizontal heterogeneities has a great effect on fog formation and development.

The French Fog Research Group set itself the goal of perfecting a numerical method for predicting dense fog, suitable for a region with high horizontal homogeneity and where during the winter season most surfaces correspond to bare soils—Nord-Pas de Calais region (no relief, monoculture, etc.).

The method described here is inspired by that used by Musson-Genon (1987): use of a 1D model forced by mesoscale terms (geostrophic wind and horizontal temperature and humidity gradient) derived from a meteorological forecasting model.

The 1D model used in our work is derived from Estournel's nocturnal boundary layer model (Estournel 1988), which had been successfully tested under conditions of nocturnal vertical stability. The sensitivity study described here has shown that two conditions are indispensable for accurate fog forecasting: the availability of good initial conditions and the values of the different parameters affecting the rate of nocturnal cooling of the atmosphere.

Our sensitivity study has enabled us to study the influence of uncertainty in the forcing parameters of the 1D model on fog forecasting (time of formation and development of fog). Here are the conclusions of this study.

(a) The choice of initial conditions is decisive for fog prediction. We chose to initialize the model with neutral conditions; in this case one needs to know the height of the mixed layer and the temperature and humidity values. We have seen that the height of the mixing layer is not critical. On the other hand it is more important to know the initial relative humidity.

(b) Four external parameters affect the atmospheric cooling rate: the geostrophic wind, the cloud cover, the soil conductivity, and the advection. The action of these parameters will be less significant for fogs that form at

the beginning of the night because of the strong local cooling during this time. The advection effect appears to us to be the most significant one to retain, since it has an effect on both the time of fog formation and its vertical development. We also showed that, in all cases, the time of fog formation is very sensitive to the presence of low clouds.

(c) Measurements taken in fog lead to gravitational settling values that are most often between 1.5 and 2  $\text{cm s}^{-1}$ . The tests conducted show that the results obtained vary little within this range of values.

(d) It is indispensable to take dew deposition into account. It is often the dew deposition that determines the time of fog formation.

This sensitivity study made it possible to determine the necessary precision for initial conditions and model forcing parameters in order to achieve accurate fog predictions. In the light of the results, one might imagine that this prediction is an impossible goal given the number of parameters that need to be known. To answer this question the model has to be tested on real cases. Simulations of cases observed during the Lille 88 field experiment will be described in Part II.

*Acknowledgments.* This study was performed as part of the Fog Project supported by the Centre National de la Recherche Scientifique (C.N.R.S.), Météo-France, and Nord-Pas de Calais region. The authors thank Jacqueline Duron and Serge Prieur (Laboratoire d'Aérodynamique) for their computing assistance. The comments from the anonymous reviewers greatly improved the quality of this paper; their effort is gratefully acknowledged.

#### REFERENCES

- Ballard, S. P., B. W. Golding, and R. N. B. Smith, 1991: Mesoscale model experiment forecasts of the Haar of northeast Scotland. *Mon. Wea. Rev.*, **119**, 2107–2123.
- Bougeault, P., and J. C. Andre, 1986: On the stability of the three order turbulence closure for the modeling of stratocumulus-topped boundary layer. *J. Atmos. Sci.*, **43**, 1574–1581.
- Brown, R., and W. T. Roach, 1976: The physics of radiation fog. Part II: A numerical study. *Quart. J. Roy. Meteor. Soc.*, **102**, 335–354.
- Corradini, C., and G. Tonna, 1980: The parameterization of the gravitational water flux in fog model. *J. Atmos. Sci.*, **37**, 2535–2559.
- Delage, Y., 1974: A numerical study of the nocturnal atmospheric boundary layer. *Quart. J. Roy. Meteor. Soc.*, **100**, 351–364.
- Durrant, D. R., and J. B. Klemp, 1982: On the effects of moisture on the Brunt-Väisälä frequency. *J. Atmos. Sci.*, **39**, 2152–2158.
- Duykerke, P. G., 1991a: Radiation fog: A comparison of model simulation with detailed observations. *Mon. Wea. Rev.*, **119**, 324–341.
- , 1991b: Observation of a quasi-periodic oscillation due to gravity waves in a shallow radiation fog. *Quart. J. Roy. Meteor. Soc.*, **117**, 1207–1224.
- Estournel, C., 1988: Etude de la phase nocturne de la couche limite atmosphérique. These doctorat d'Etat n° 1361, Université Paul Sabatier, Toulouse, France, 161 pp.
- , and D. Guedalia, 1985: Influence of geostrophic wind on atmospheric nocturnal cooling. *J. Atmos. Sci.*, **42**, 2695–2698.

- , and —, 1987: A new parameterization of eddy diffusivities for nocturnal boundary layer modeling. *Bound.-Layer Meteor.*, **39**, 191–203.
- Fitzjarrald, D. R., and G. G. Lala, 1989: Hudson Valley fog environment. *J. Appl. Meteor.*, **28**, 1303–1328.
- Gertler, A. W., and R. L. Steele, 1980: Experimental verification of the linear relationship between IR extinction and liquid water content of clouds. *J. Appl. Meteor.*, **19**, 1314–1317.
- Guedalia, D., and T. Bergot, 1992: Premiers resultats de la campagne Lille 88 d'etude du brouillard. *Meteorologie*, **42**, 11–20.
- , J. Moneris, P. Sarthou, R. Vehil, R. Serpolay, J. L. Casanova, R. San Jose, and R. Vilorio, 1989: La campagne Valladolid 85 d'etude du brouillard: Deroulement et premiers enseignements. *Meteorologie*, **26**, 24–32.
- Justo, J. E., and G. Lala, 1980: Radiation fog formation and dissipation: A case study. *J. Rech. Atmos.*, **14**, 391–397.
- , and —, 1983: Radiation fog fields programs. Recent studies. ASRC-SUNY Publication 869, 67 pp.
- Kunkel, B., 1984: Parameterization of droplet terminal velocity and extinction coefficient in fog model. *J. Appl. Meteor.*, **23**, 34–41.
- Lala, G. G., J. E. Justo, M. B. Meyer, and M. Kornfein, 1982: Mechanisms of radiation fog formation on four consecutive nights. *Proc. Conf. on Clouds Physics*, Chicago, Amer. Meteor. Soc., 9–11.
- Moneris, J., 1989: Etude d'une couche de brouillard: observations et simulations numeriques. These de doctorat de l'Universite Paul Sabatier n° 409, Toulouse, France, 136 pp.
- Musson-Genon, L., 1987: Numerical simulations of a fog event with a one-dimensional boundary layer model. *Mon. Wea. Rev.*, **115**, 592–607.
- Noilhan, J., and S. Planton, 1989: A simple parameterization of land surface processes for meteorological model. *Mon. Wea. Rev.*, **117**, 536–549.
- Pielke, R. A., 1984: *Mesoscale Meteorological Modeling*. Academic Press, 612 pp.
- Pinnick, R. G., D. L. Hoihjelle, G. Fernandez, E. B. Stenmark, J. D. Lindberg, G. B. Hoidale, and S. G. Jennings, 1978: Vertical structure in atmospheric fog and haze and its effects on visible and infrared extinction. *J. Atmos. Sci.*, **35**, 2020–2032.
- Roach, W. T., 1976: On some quasi-periodic oscillations observed during a field investigation of radiation fog. *Quart. J. Roy. Meteor. Soc.*, **102**, 355–359.
- , R. Brown, S. J. Caughey, J. A. Garland, and C. J. Readings, 1976: The physics of radiation fog. Part I: A field study. *Quart. J. Roy. Meteor. Soc.*, **102**, 313–333.
- , —, —, B. A. Crease, and A. Slingo, 1982: A field study of nocturnal stratocumulus. I: Mean structure and budgets. *Quart. J. Roy. Meteor. Soc.*, **108**, 103–123.
- Therry, G., and P. Lacarrere, 1983: Improving the eddy kinetic energy model for planetary boundary layer description. *Bound.-Layer Meteor.*, **25**, 63–88.
- Turton, J. D., and R. Brown, 1987: A comparison of a numerical model of radiation fog with detailed observations. *Quart. J. Roy. Meteor. Soc.*, **113**, 37–54.
- Vehil, R., J. Moneris, D. Guedalia, and P. Sarthou, 1989: Study of the radiative effects within a fog layer. *Atmos. Res.*, **23**, 179–194.
- Yamada, T., 1983: Simulations of nocturnal drainage flows by a  $q^2l$  turbulence closure model. *J. Atmos. Sci.*, **40**, 91–106.
- Zdunkowski, W., and B. Nielsen, 1969: A preliminary prediction analysis of radiation fog. *Pure Appl. Geophys.*, **19**, 45–66.
- , and A. Barr, 1972: A radiative-conductive model for the prediction of radiation fog. *Bound.-Layer Meteor.*, **3**, 152–157.